Title

Spatiotemporal tissue maturation of thalamocortical pathways in the human fetal brain

Authors

Siân Wilson[1,2], Maximilian Pietsch[1], Lucilio Cordero-Grande[1,3,4], Daan Christiaens[1,5], Alena Uus[6], Vyacheslav Karolis[1], Vanessa Kyriakopoulou[1], Kathleen Colford[1], Anthony N. Price[1], Jana Hutter[1], Mary A. Rutherford[1], Emer J. Hughes[1], Serena J. Counsell[1], Jacques-Donald Tournier1, Joseph V Hajnal[1], A. David Edwards[1,2], Jonathan O'Muircheartaigh*[1,2,7,8], Tomoki Arichi*[1,2, 9,10]

*joint last author

Affiliations

1. Centre for the Developing Brain, School of Biomedical Engineering and Imaging Sciences, King's College London, London, SE1 7EH, United Kingdom;
2. Centre for Neurodevelopmental Disorders, Kings College London, London, SE1 1UL, United Kingdom;
3. Biomedical Image Technologies, ETSI Telecomunicación, Universidad Politécnica de Madrid, 28040 Madrid, Spain;
4. Biomedical Research Networking Center in Bioengineering, Biomaterials and Nanomedicine (CIBER-BBN), 28029 Madrid, Spain;
5. Department of Electrical Engineering (ESAT/PSI), Katholieke Universiteit Leuven, 3001 Leuven, Belgium;
6. Department of Biomedical Engineering, School Biomedical Engineering and Imaging Sciences, King's College London, St. Thomas' Hospital, London, United Kingdom
7. Department of Forensic and Neurodevelopmental Sciences, King's College London, London SE5 8AF, United Kingdom;
8. Department of Neuroimaging, Institute of Psychiatry, Psychology and Neuroscience, King's College London, London SE5 8AF, United Kingdom
9. Children's Neurosciences, Evelina London Children's Hospital, Guy's and St Thomas' NHS Foundation Trust, London SE1 7EH, United Kingdom;
10. Department of Bioengineering, Imperial College London, London SW7 2AZ, United Kingdom

Abstract

The development of connectivity between the thalamus and maturing cortex is a fundamental process in the second half of human gestation, establishing the neural circuits that are the basis for several important brain functions. In this study, we acquired high-resolution *in utero* diffusion MRI from 140

fetuses as part of the Developing Human Connectome Project, to examine the emergence of thalamocortical white matter over the second to third trimester. We delineate developing thalamocortical pathways and parcellate the fetal thalamus according to its cortical connectivity using diffusion tractography. We then quantify microstructural tissue components along the tracts in the fetal compartments that are critical substrates for white matter maturation, such as the subplate and intermediate zone. We identify patterns of change in the diffusion metrics that reflect critical neurobiological transitions occurring in the second to third trimester, such as the disassembly of radial glial scaffolding and the lamination of the cortical plate. These maturational trajectories of MR signal in transient fetal compartments provide a normative reference to complement histological knowledge, facilitating future studies to establish how developmental disruptions in these regions contribute to pathophysiology.

Introduction

Thalamocortical connections represent the most important inputs into the developing cortex during the second half of human gestation, where they play a key role in guiding cortical areal differentiation and establishing the circuitry responsible for sensory integration across the lifespan (Jones 2007; Price et al. 2006; Schummers, Sharma, and Sur 2005; Sharma, Angelucci, and Sur 2000; Sur and Rubenstein 2005). Their importance is highlighted by previous work implicating disruptions to thalamocortical development during the perinatal period in the pathophysiology of neurodevelopmental disorders such as schizophrenia (Klingner et al. 2014; Marenco et al. 2012) bipolar disorder (Anticevic et al. 2014), and autism (Nair et al. 2013). Altered thalamocortical connectivity has also been described in preterm infants, and was used to predict cognitive outcome (Ball et al. 2013, 2015; Toulmin et al. 2021), highlighting the specific vulnerability of these pathways during the second to third trimester. Although thalamocortical development has been studied in animals (Brody et al. 1987; Ivica Kostović and Jovanov-Milošević 2006; Molnár and Blakemore 1995; Yakovlev et al. 1960) and post-mortem human tissue (Krsnik et al. 2017; Takahashi et al. 2012; Wilkinson et al. 2017) little is known about *in vivo* white matter maturation during fetal development.

White matter development in the late second and third trimesters of human gestation (between 21 and 37 weeks) is characterised by a sequence of precisely timed biological processes occurring in transient compartments of the fetal brain (I. Kostović and Judaš 2015; Ivica Kostović and Judaš 2010). These processes include the migration of neurons along the radial glial scaffold, accumulation of thalamocortical axons in the superficial subplate, innervation of the target cortical area, conversion of radial glial cells into astrocytes, and ensheathment of axonal fibres (Krsnik et al 2017, Molliver et al. 1973; Kostovic and Molliver 1974; Kostovic and Goldman-Rakic, 1983, 1984,1990; Kostovic´ and Judasˇ 2002, 2006, 2007, 2010). The challenge for *in vivo* neuroimaging studies is to disentangle the effect of these different neurobiological processes on the diffusion MRI signal, to improve mechanistic insight about the transformation of transient fetal compartments into segments of developing white matter (Kostovic 2012).

Recent advances in diffusion weighted imaging now allow *in vivo* characterization and estimation of white matter development during the fetal period. Tractography has been used to estimate the fetal brain's major white matter bundles and quantitatively characterise the evolution of the microstructure across the second half of gestation (Bui et al. 2006; Jaimes et al. 2020; Jakab et al. 2015; Keunen et al. 2018; Khan et al. 2019; Lockwood Estrin et al. 2019; Machado-Rivas et al. 2021; Wilson et al. 2021; Zanin et al. 2011). Advanced acquisition and analysis methods enable the relative contribution of constituent tissue and fluid compartments to the diffusion signal to be estimated (Jeurissen et al. 2014; Pietsch et al. 2019). Using this approach, previous work has identified non-linear trends in diffusion metrics over the second to third trimester (Wilson et al., 2021). Namely, we observed an initial decrease in tissue fraction within developing white matter between 22 and 29W, which could be due to the radial glial scaffold disassembling (Rakic 2003). Subsequently, we observed an increase from 30 to 36W, potentially linked to more coherent fibre organisation, axonal outgrowth and ensheathment (Back 2002, Haynes 2005, Wimberger 1995), increasing the structural integrity of maturing white matter. Interpreting these trends is especially challenging in the rapidly developing fetal brain, because of the high sensitivity and low specificity of diffusion metrics to various co-occurring biological processes.

We hypothesise that the biological processes occurring in different fetal compartments leads to predictable changes in diffusion metrics along tracts, reflecting the appearance and resolution of these transient zones. When a mean value across the whole-tract is calculated, sensitivity to the unique neurobiological properties of each transient compartment is lost. For example, in the early prenatal and mid prenatal period, the subplate is a highly water-rich compartment containing extracellular matrix, whereas the cortical plate and the deep grey matter are relatively cell dense (Kostovic 2010). We therefore predict that the tissue fraction would be higher in the deep grey matter and the cortical plate and lower in the subplate. We investigate this by characterising the entire trajectory of tissue composition changes between the thalamus and the cortex, to explore the role of transient fetal brain developmental structures on white matter maturational trajectories.

We acquired diffusion weighted imaging from 140 fetuses over a wide gestational age (GA) range (21 to 37W) and use tractography to delineate five distinct thalamocortical pathways. To investigate whether the immature axonal bundles can be traced back to specific and distinct locations within thalamus, we parcellate the thalamus according to streamline connectivity (Behrens et al., 2003). We find consistent and distinct origins of different tracts, resembling the adult topology of thalamic nuclei (Toulmin et al., 2015, Behrens et al., 2003) as early as 23W gestation. We then apply a multi-shell multi-tissue constrained spherical deconvolution (MSMT-CSD) diffusion model (Jeurissen et al, 2014) and derive tissue and fluid fraction values, charting tract-specific maturational profiles over the second to third trimester. We overlay the tracts on an atlas of transitioning fetal compartments and correlate changes in the diffusion MRI signal across time with critical neurodevelopmental processes, such as the dissolution of the subplate and lamination of the cortical plate. We demonstrate that along-tract sampling of diffusion metrics can capture temporal and compartmental differences in the second to third trimester, reflecting the maturing neurobiology of the fetal brain described in histology studies. With these methods, we provide a detailed, accurate reference of the unique developing microstructure in each tract that improves mechanistic insight about fibre maturation, bridging the gap between MRI and histology.

122

Results

Estimating thalamocortical pathways using probabilistic streamline tractography

High-angular-resolution multi-shell diffusion weighted imaging (HARDI) was acquired from 140 fetuses between 21 and 37 gestational weeks (70 male, 70 female) as part of the Developing Human Connectome Project (dHCP). Data were corrected for fetal head motion and other imaging artefacts (Christiaens et al, 2021). Individual subject orientation density functions (ODFs) were then computed using cohort-specific fluid and "tissue" response functions and compiled to generate weekly diffusion templates (see Methods). The diffusion templates were then registered to a T2-weighted brain atlas (Gholipour et al. 2017) of tissue segmentations, used to generate anatomically constrained whole-brain connectomes for each gestational week (Smith et al. 2012; Tournier et al. 2019). To constrain our investigation, we selected thalamocortical pathways that are at a critical stage in their development and are vulnerable to external influences in the second to third trimester (Batalle et al. 2017; Nosarti et al. 2014; Raybaud et al. 2013), the anterior thalamic radiation (AT), thalamic-motor tract (TM), thalamic-sensory tract (TS), posterior parietal tract (PP) and optic radiation (OR) . The connectomes were filtered down to the pathways of interest using inclusion regions defined by the T2 atlas, including the thalamus and specific cortical areas (Figure 1). These included the primary motor cortex, primary sensory cortex, posterior parietal cortex, dorso-lateral prefrontal cortex, and the primary visual cortex. With this method, we were able to delineate five major thalamocortical pathways in each gestational week. To keep regions of interest more consistent across the cohort, we grouped all cases into two-weekly intervals, starting at 23w (Figure 2), replicating methods used previously (Wilson et al., 2021).

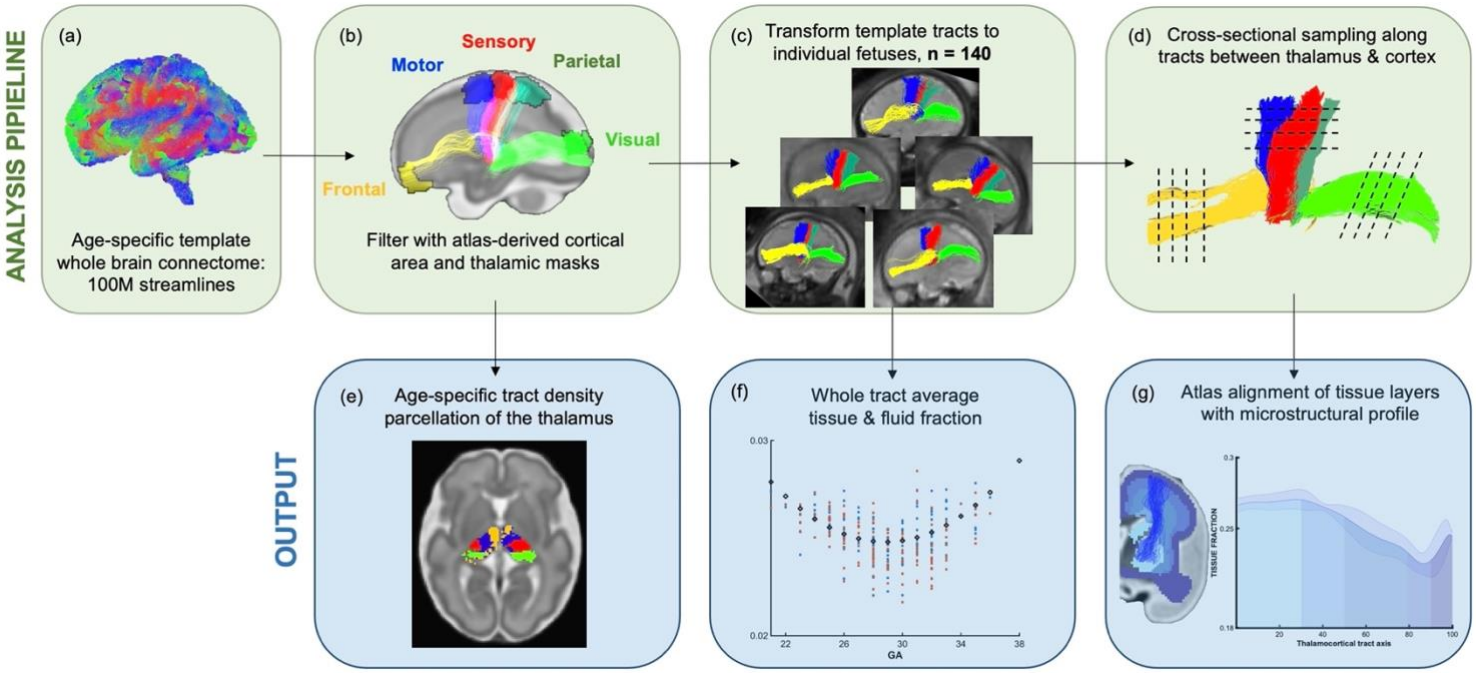

Figure 1. Methods pipeline to estimate and quantify thalamocortical tracts development. *(Top Row) (a) Whole brain connectomes generated for each gestational week template. (b) Atlas-defined masks of the thalamus and cortical areas were used to extract white matter pathways of interest from the connectomes. (c) These pathways were transformed to the native fetal diffusion space, (d) the values were sampled along the tract. (f) Whole-tract average diffusion metrics were calculated or (g) values sampled along the tract were aligned to an atlas of transient fetal compartments.*

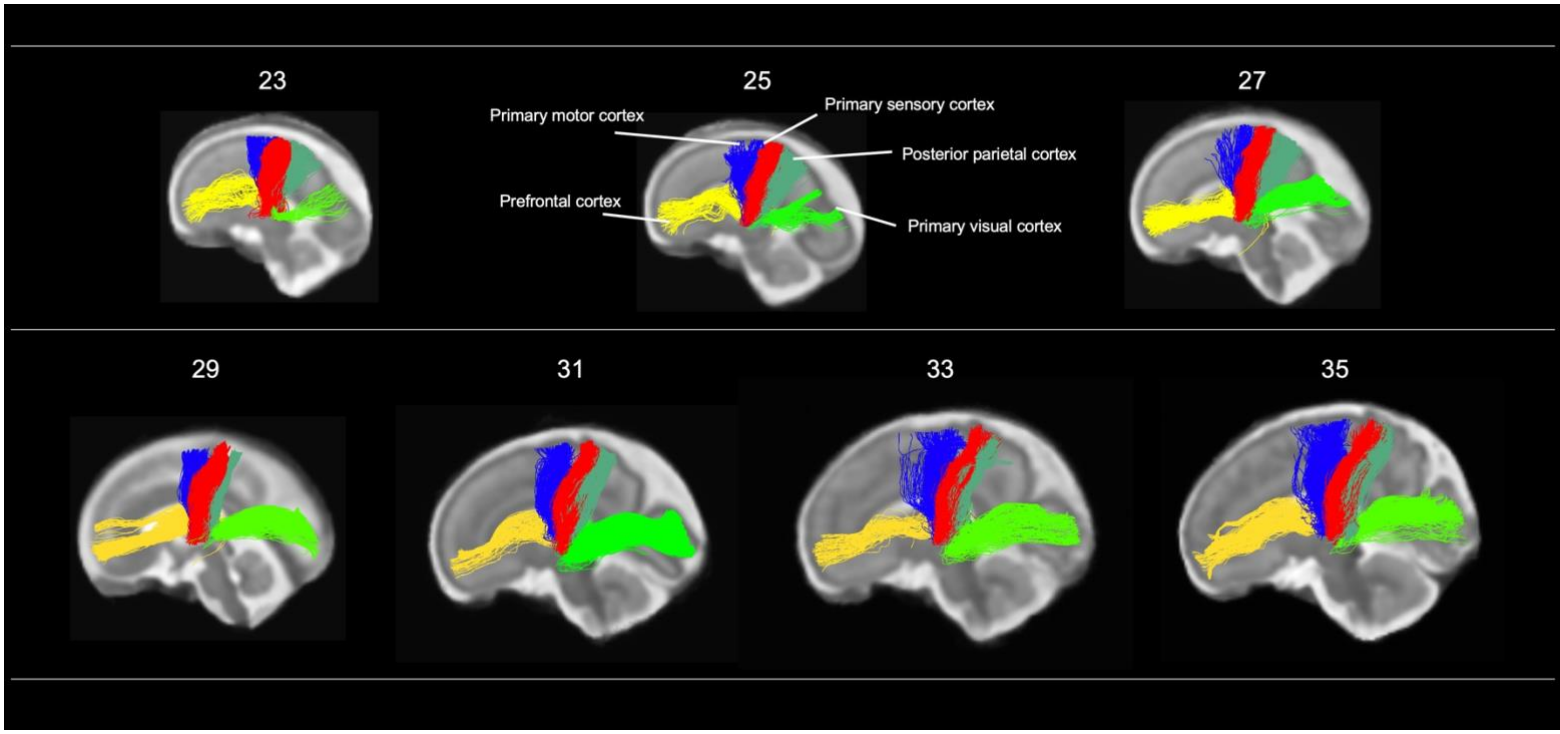

Figure 2. *Tractography of thalamocortical pathways in different gestational week templates across the second to third trimester. Tracts project to 5 different cortical areas, the primary motor cortex, (blue) primary sensory cortex (red), posterior parietal cortex (teal), prefrontal cortex (yellow) and primary visual cortex (bright green).*

Structural connectivity parcellation of the fetal thalamus resembles adult topology of thalamic nuclei

Tract density imaging (Calamante 2010) was used in each ODF template to explore whether the different cortical areas were connected to distinct, specific regions of the thalamus (Figure 3a). We found that for all ages, there was symmetrical topographical representation of the cortical regions of interest in the thalamus. Furthermore, they spatially corresponded to the adult organisation of thalamic nuclei, demonstrated by the schematic (Figure 3a) which is based on Morel's thalamus and other connectivity derived parcellations from adult imaging studies (Morel, Magnin, and Jeanmonod 1997; Najdenovska et al. 2018; Niemann et al. 2000). The tract projecting to the prefrontal cortex was connected to the anterior thalamus and in the younger ages (23-29W) also to the medial thalamus. In

170 the older templates (31, 33 and 35W), frontal connectivity was more localised to the anterior thalamus
171 and less evident in the medial area. There were distinct but neighbouring areas in the ventral thalamus
172 connecting to the sensory and motor cortical areas, the motor-connected thalamic region being more
173 frontal. The connectivity of the posterior parietal area was in the posterior part of the thalamus, and the
174 most posterior voxels in the thalamic mask projected to the primary visual cortex.
175

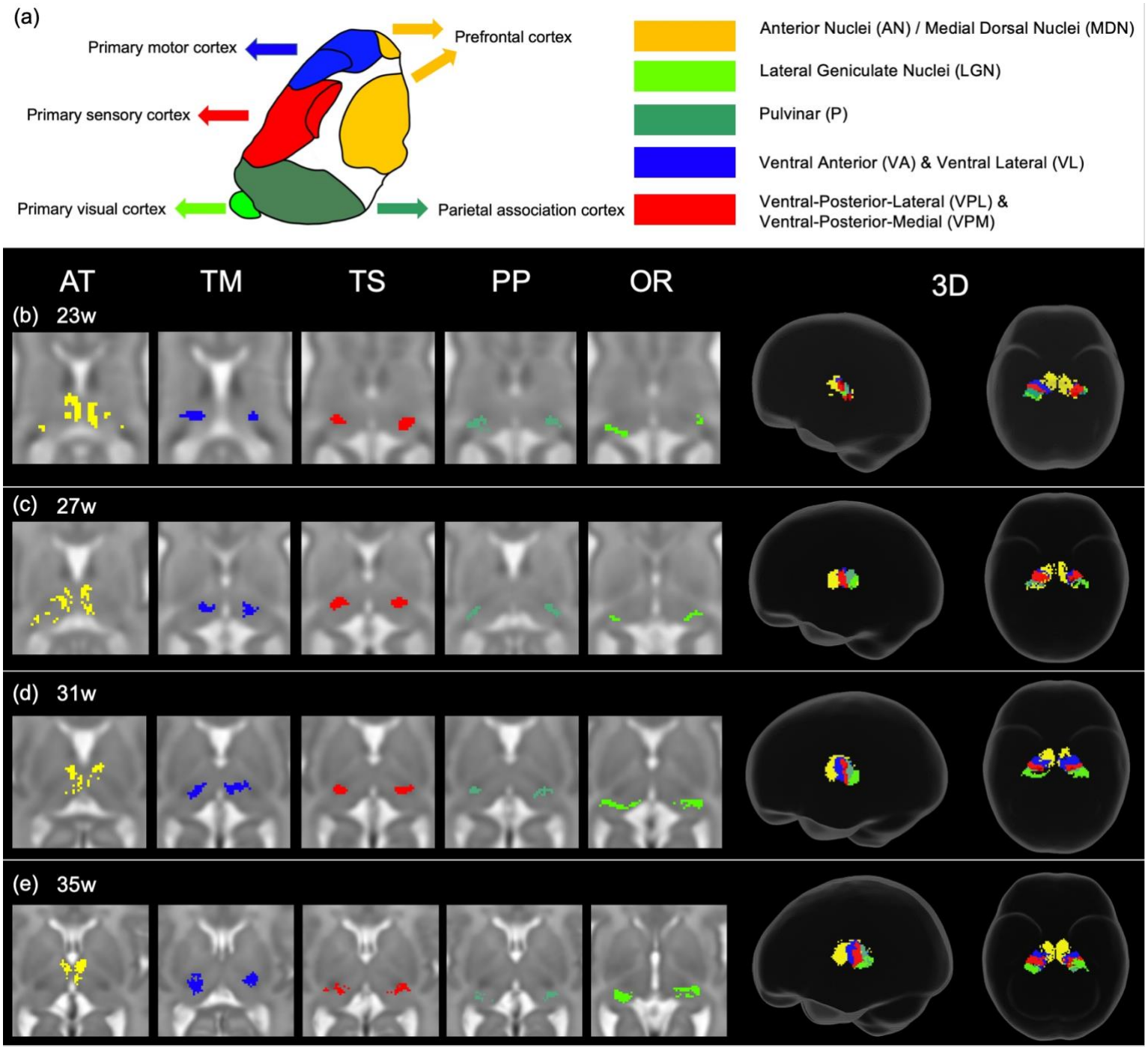

176

Figure 3. Tract-density imaging parcellation of at different fetal ages (a) *A schematic of expected cortical connectivity arrangement across the thalamus, based on Morel's parcellation of the adult thalamic nuclei (b) Axial slices of thalamic parcellation, thresholded for the top 20% of voxels, colour-coded according to streamline connectivity of different tracts at 23w, (c) 27w (d) 31w and (e) 35w.*

Whole-tract average diffusion metrics have a characteristic U-shaped trend across the second to third trimester

The thalamocortical pathways were transformed from the age-matched templates to the native subject space for 140 fetal subjects (Figure 4a). The MSMT-CSD-derived voxel-average tissue and fluid ODF values were sampled along the warped group-average streamline tracts. Tract-specific values were derived by averaging these for each tract in each subject, replicating the approach that has been used in previous fetal studies (Wilson et al., 2021). The values for each tract were plotted against the GA of the subject. The Akaike Information Criterion (AIC) suggested second order polynomial relationships for all tracts for both tissue and fluid fraction metrics, except the fluid fraction in the AT which is linear (Figure 4b).

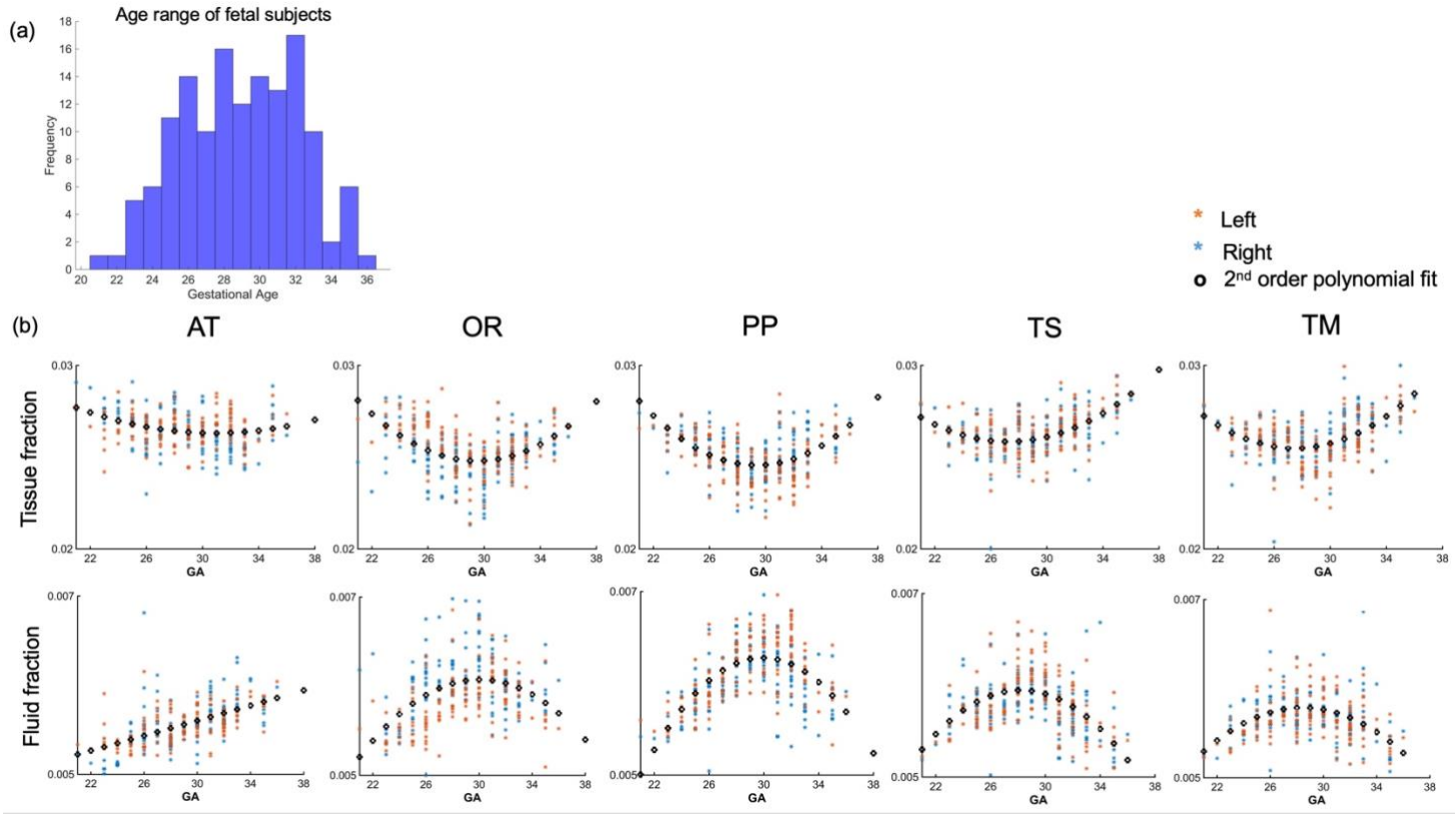

194

195 ***Figure 4. Diffusion metric age-trajectories for each tract*** *(a) Distribution of age among the fetal cohort*
196 *in gestational weeks. (b) Whole-tract average tissue (top) and fluid fractions (bottom) for each subject*
197 *in the left (orange) and right (blue) hemisphere, plotted against gestational age (GA) of the subject,*
198 *best fit by 2nd order polynomials. (AT = anterior thalamic radiation, OR = optic radiation, PP =*
199 *posterior parietal tract, TS = thalamic-sensory tract, TM = thalamic-motor tract).*

200

201

202 **Along-tract sampling reveals evolving properties of fetal brain transient compartments**

203

204 To explore the origins of these trends in diffusion metrics, the values of tissue and fluid fraction were
205 sampled in subject-space at 100 equidistant intervals between the thalamus and the cortex. Tissue and
206 fluid fraction are scaled jointly per scan such that they are approximately reciprocal of one another
207 across the brain using a cubic polynomial spatial model (Pietsch et al. 2019). In each subject, we
208 sampled the tissue and fluid fraction values beneath the streamlines from the thalamus to the cortex,

209 plotting the microstructural tissue composition against the distance from the thalamus (Figure 5). We
210 found that trajectories changed gradually between gestational weeks, and therefore we grouped them to
211 match previous histology studies that define this fetal period according to three developmental
212 windows, early (21-25.5w), mid (26-31.5w) and late (32-36w) prenatal period (Kostovic, Vasung et al
213 2020) (see supplementary info). When comparing the microstructural profiles of all the tracts in the
214 different periods, the motor, sensory and parietal tracts shared similar trajectories, whilst those in the
215 anterior thalamic and optic radiation tracts were more distinct (Figure 5a, b, c and Supplementary Figure
216 1(a) and (b)).
217
218 To improve our ability to corroborate changes in the diffusion MRI signal with observations from
219 histological studies, we mapped the maturational trajectories to an atlas of fetal brain compartments
220 (Gholipour et al. 2017) and overlayed the boundaries of these compartments on the tissue and fluid
221 fraction trajectories (Figure 5). Tissue fraction values in the deep grey matter and the cortical plate areas
222 increased with gestational age in all tracts. This increase was most marked in the tracts terminating in
223 superior areas of the brain (motor, sensory and superior parietal cortex) (Figure 5(a) TM, Supplementary
224 Figure 1(a) TS and (b) PP). The tissue fraction of the ventricular and intermediate zones decreased
225 between the early and mid-prenatal period, in all tracts. This decrease was very pronounced in the motor,
226 sensory and superior parietal tracts. The subplate tissue fraction changes were more tract specific. In
227 the subplate of sensorimotor and parietal tracts, there was initially a very high fluid fraction and low
228 tissue fraction, which transitions across the second to third trimester, increasing in tissue fraction from
229 early to mid and then to late prenatal. Whereas in the anterior thalamic radiation, there was a decrease
230 in subplate tissue fraction with GA (and a reciprocal increase in fluid fraction). In the optic radiation,
231 the subplate tissue fraction decreases between early and mid-prenatal to then increase again in late
232 prenatal. Highest tissue fractions were generally observed in the ventricular zone, with the lowest tissue
233 fraction in the subplate area.
234

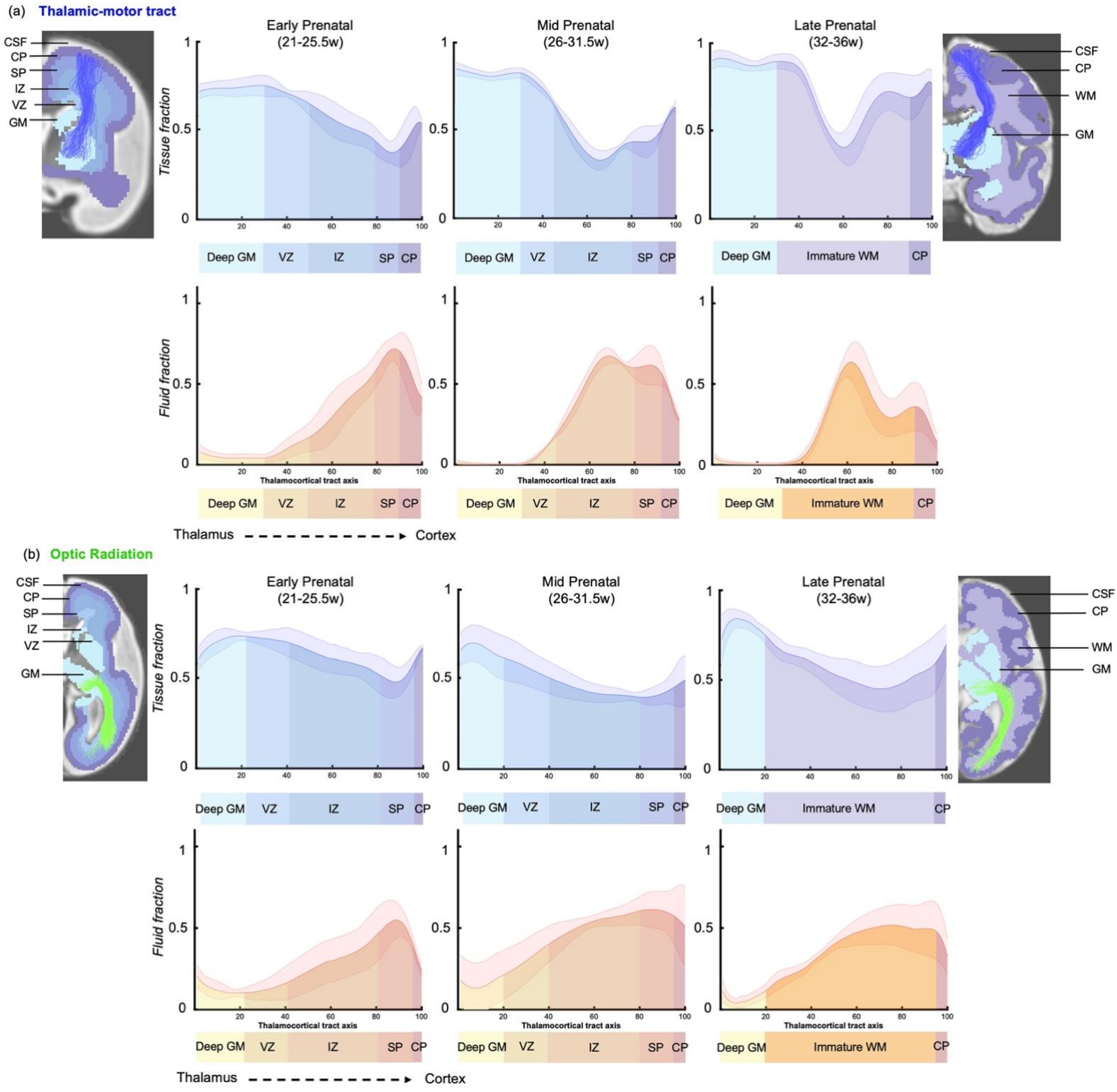

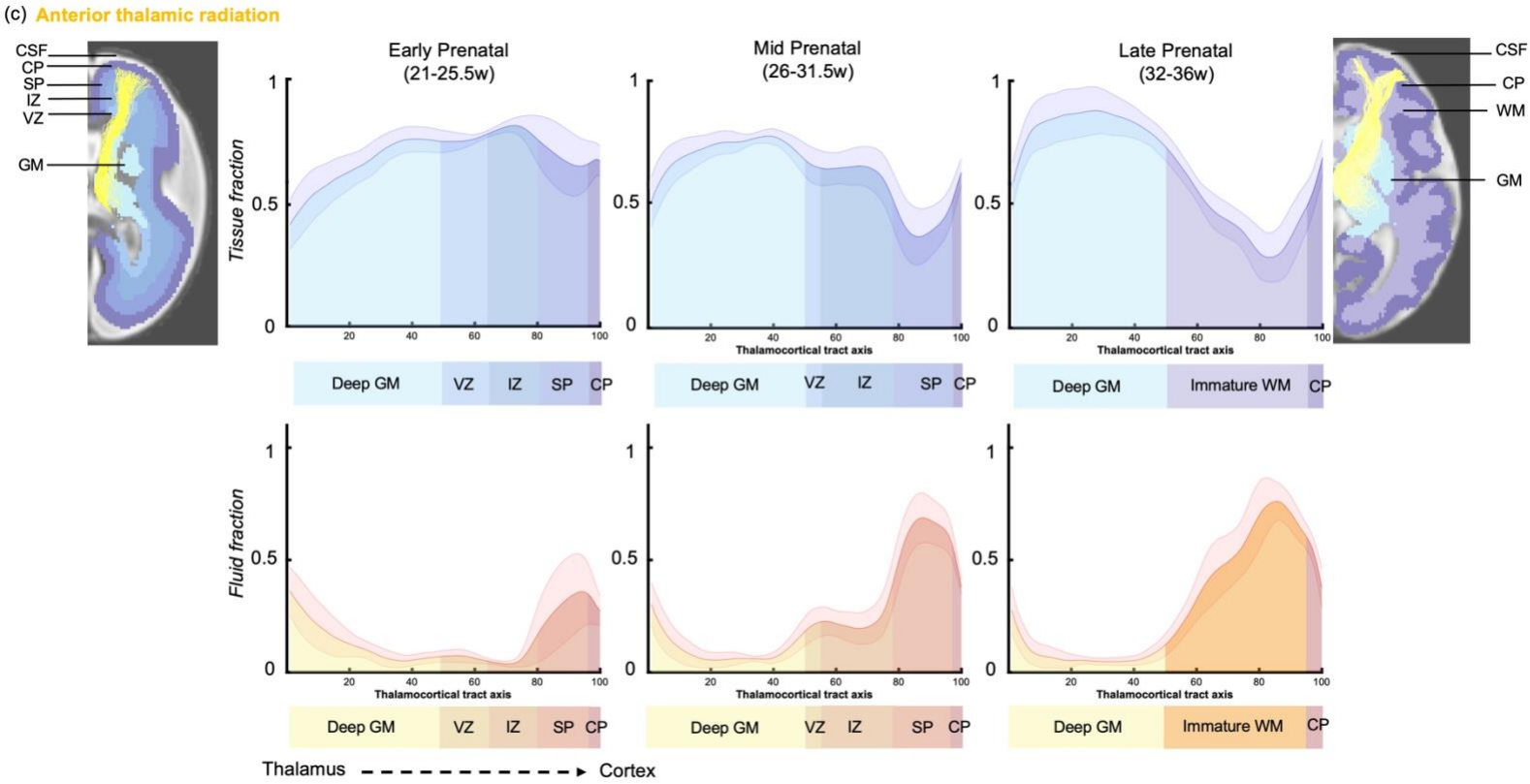

Figure 5. Microstructural composition of fetal compartments traversed by developing thalamic white matter. *Tracts were overlayed on the atlas of fetal compartments (examples highlight the difference between fetal brain structure in early prenatal (25w) on far left, and late prenatal (35w) on far right). Tissue fraction trends (top row) and fluid fraction trends (bottom row), normalised to 1, between the thalamus and cortex (thalamocortical tract axis) for the (a) Thalamic-motor tract, (b) Optic radiation and (c) Anterior thalamic radiation. Subjects were grouped by age, and average trajectories plotted for early prenatal (22-25.5w), mid prenatal (26-31.5w), late prenatal (32-36w). Error bars represent the standard deviation among all subjects in each group. Atlas-derived tissue boundaries are marked on the trajectories to reveal the changing tissue properties of each layer between early, mid and late prenatal development. (Cortical spinal fluid = CSF, Cortical plate = CP, Subplate = SP, Intermediate zone = IZ, Ventricular zone = VZ, Deep grey matter = GM, Immature white matter = WM).*

Discussion

In this work, we studied *in utero* development of five distinct thalamocortical pathways using state-of-the-art diffusion MR imaging methods and bespoke pre-processing pipeline (Christiaens et al. 2019; Cordero-Grande et al. 2019; Hutter, Christiaens, et al. 2018; Pietsch et al. 2019; Wilson et al. 2021) in 140 fetuses aged 21 to 37 weeks gestation. We show that these pathways connect to distinct thalamic nuclei, which could be clearly defined at group level even at 23W. To disentangle the impact of different neurobiological processes on diffusion metrics, we characterized the tissue composition profile along each of the thalamocortical tracts as they traverse the different developmental tissue layers of the fetal brain. We found the spatiotemporal changes in the diffusion signal reflected known developmental processes that take place between the early, mid and late prenatal period. The early period is characterized by higher tissue fractions in the middle of the tract, where there is a radial scaffold for migrating neurons. As this scaffold dissipates in the mid prenatal period, this is accompanied by a reduction in the tissue fraction in the middle of the tract, and an increase in towards the termination of the tracts as the neurons of the cortical plate mature. Finally in the late prenatal period, we observe the highest tissue fraction values at the start and end of the axis, as the premyelination phase of white matter development commences. This study demonstrates how the diffusion MRI signal can be modelled to create *in vivo* spatiotemporal trajectories which relate to underlying neurobiological properties and are consistent with described trends from post-mortem histology (Kostovic, Progress in Neurobiology 2020).

Early embryonic patterning of gene expression and cell division in the thalamus provide a template for specialised nuclei to emerge over the course of development, such that specific cells eventually occupy distinct locations within the thalamus (Clascá, Rubio-Garrido, and Jabaudon 2012; Nakagawa 2019) Thalamocortical tracts emerge over the same timescale as the thalamus parcellates and matures into its specialised group of nuclei (Clascá, Rubio-Garrido, and Jabaudon 2012). Although the topography of thalamic nuclei and their cortical connectivity is acquired embryonically, no *in vivo* parcellation of the thalamus in the fetal brain has been published. Using tract density imaging, we observed that the cortical areas were connected to specific thalamic regions, organised in an anterior-posterior axis. This anterior-posterior representation of cortical connectivity in the thalamus was consistent across the second to

third trimester and is in accordance with the topology of thalamic nuclei described in animal studies and histology (Molnar & Blakemore, 1995; Molnar et al., 1998a, b). In addition, our fetal structural connectivity parcellation resembles the functionally-derived thalamic parcellation in neonates, supporting the view that there is a strong association between structure and function in thalamocortical circuitry that begins early in life (Johansen-Berg 2005, Toulmin 2015, Alcauter 2014). It is worth noting that this thalamic parcellation is dependent on streamline count through a voxel, and in the fetal brain streamlines are prone to spurious detection. Particularly in the youngest fetuses, where we observe an extremely dense connectome (due to a fixed number of streamlines in a smaller brain) but there are very few coherent axonal bundles, tracts might be overrepresented in the thalamic parcellation.

Recent studies characterising developing white matter pathways using human fetal MRI identified 2nd order polynomial maturational trends in diffusion metrics unique to this developmental period (Wilson et al., 2021, Machado-Riveras et al., 2021). Here we replicated these methods with a different group of tracts and found the same U-shaped trends in thalamocortical white matter development. The inflection point at around 29-30w was hypothesised to be the result of the dissipating radial glial scaffold followed by the pre-myelination phase of white matter development (Wilson et al,, 2021, Machado-Riveras et al., 2021). The sensitivity of HARDI to radially organised structure in the fetal brain has been described by previous studies (Miyazaki, Song, and Takahashi 2016; Takahashi et al. 2012; Xu et al. 2014) combining it with post-mortem tissue analysis to show that radially coherent diffusion signal corresponded to radial glial fibres in the early prenatal period, transitioning to cortico-cortical fibres around 30 weeks, coinciding with the appearance of astrocytes (Takahashi et al. 2012; Xu et al. 2014). However, with whole-tract average values, it is not possible to establish the precise effect of different neurodevelopmental processes on diffusion metrics across gestation.

To address this ambiguity, we characterised the entire trajectory of tissue composition changes between the thalamus and the cortex. We found that age-related changes in the tissue and fluid fraction along the tracts concurred with histological observations (Ivica Kostović and Judaš 2010). During the early prenatal period (22 - 25.5 GW), neuronal precursors migrate along the radial glial scaffold from

proliferative zones to their destination in the cortical plate and thalamocortical axons accumulate in the superficial subplate, entering a "waiting phase", forming transient synaptic connections (Ghosh et al. 1990; I. Kostovic and Rakic 1984; Ivica Kostovic and Goldman-Rakic 1983; Ivica Kostovic and Rakic 1990a). In terms of the diffusion signal, this strongly aligned microstructure of the radial glia is represented in our results by a higher tissue fraction in the transient compartments containing the most migratory cells (such as the VZ, IZ) (Ivica Kostović and Judaš 2010). Conversely, we observe the lowest tissue fraction in the early prenatal SP, as this compartment predominantly contains hydrophilic extracellular matrix (Allendoerfer and Shatz 1994; Miller et al. 2014; Bakken et al. 2016; Molnár and Hoerder-Suabedissen 2016).

By the mid prenatal period (26w-31.5w), we observe increased tissue fraction in the cortical plate, coinciding with the innervation of the cortical plate by thalamocortical axons, increasing soma volume and dendritic branching of CP neurons and CP synaptogenesis (Huttenlocher and Dabholkar 1997; Peter R. 1979; zljak et al. 1992). We also observe increased tissue fraction in the SP zone in the mid prenatal period, consistent with histological observations of increased coherence of axonal fibres between cortical areas (Takahashi et al. 2012; Xu et al. 2014). The tissue fraction in the VZ and IZ decreases compared to the early prenatal period, corresponding to the timeframe when the radial glial scaffold dissipates (Back et al. 2001; Haynes et al. 2005; Kinney et al. 1988).

From the mid to late prenatal period, there is a marked increase in tissue fraction in last third of the axis between thalamus and cortex. By this point in development, the radial glia have converted into oligodendrocyte precursor cells which ensheath the axonal fibres to commence pre-myelination, enhancing the structural integrity of the fibre pathways (Back et al. 2001, 2002; Haynes et al. 2005; Kinney et al. 1988, 1994). A previous study has shown that this oligodendrocyte lineage progression correlates with diffusion metrics (Drobyshevsky et al. 2005) suggesting it is likely to contribute to the increased tissue fraction we observe in the late prenatal period. The tissue fraction increase in the CP area is consistent in time with the lamination of the CP, the elaboration of thalamocortical terminals in layer IV and a rapid growth of basal dendrites of layer III and V pyramidal neurons (Ivica Kostovic and

Goldman-Rakic 1983; Ivica Kostović and Judaš 2006; Krsnik et al. 2017; Molliver, Kostović, and Van Der Loos 1973). These high tissue fraction values at the origin and termination of the tracts suggest co-maturation between ascending and descending pathways between the thalamus and cortex to eventually form continuous, structurally mature fibre bundles. This concept was proposed in the 90's by Blakemore and Molnar, termed the "handshake hypothesis". They suggested that thalamocortical pathways ascending through the internal capsule project to their cortical targets with assistance from reciprocal descending cortical pathways (Molnár and Blakemore 1995). We hypothesise that continuing this analysis over subsequent weeks into the neonatal period, would lead to an increasing tissue fraction in the middle of the axis, as fibre bundles become more uniformly structurally mature and the subplate completely resolves (Haynes et al. 2005; Kinney et al. 1988, 1994; Ivica Kostović and Judaš 2006).

We observed that tracts terminating superiorly (motor, sensory and parietal) shared very similar trajectories in the early, mid and late periods. However, the optic radiation and the anterior thalamic radiation had more distinct trajectories. The microstructural change along the anterior thalamic radiation suggests increasing tissue fraction between the deep grey matter, VZ and IZ. We hypothesise that the high tissue fraction in the IZ is due to densely packed ascending and descending bundles within the anterior limb of the internal capsule (Emos and Agarwal 2019). On the other hand, the optic radiation traverses the deep parietal lobe along the border of the lateral ventricle and has smoother transitions in tissue fraction between the fetal compartments. This is likely due to the tract area running more parallel to the tissue interfaces. Another explanation for the regional differences in microstructural properties is the variation in subplate remnants. In the late prenatal trajectories, all tracts except the optic radiation have a large dip in tissue fraction along the tract. In the primary visual cortex, the subplate disappears during the final weeks of gestation, whereas in the somatosensory cortex there are still subplate neurons present in term-born neonates (Ivica Kostovic and Rakic 1990b) and the subplate of the pre-frontal associative cortex gradually disappears over the six postnatal months. Therefore, the peaks of fluid fraction in the frontal and sensory trajectories might reflect the lasting presence of subplate in these areas (Ivica Kostović and Judaš 2006; Ivica Kostovic and Rakic 1990a).

The methods described allow the direct study of the maturational effects of the subplate and intermediate zones, which are known to represent critical substrates for early synaptogenesis and the spatial guidance of thalamocortical axons (Ghosh et al. 1990). Damage to this essential structural framework for developing cortical circuitry has been implicated in the origins of numerous developmental disorders, and is suspected to underly the altered structural and functional connectivity of the thalamus in preterm infants (Kostovic et al. 1989; Kostovic et al. 2011; Volpe 1996, 2000; Huppi et al. 2001; Kostovic and Judas 2002, 2006, 2007, 2010; Counsell et al. 2003; McQuillen and Ferriero 2005; Hadders-Algra 2007; Mathur and Inder 2009; Kinney et al. 2012, Toulmin et al., 2015, Ball et al., 2012, Ball et al., 2015, Kostovic & Judas 2010, Volpe 2009, Toulmin cerebral cortex). It is therefore critical to use clinically relevant tools, such as in utero MRI, to relate the microstructural properties of these transient fetal compartments to neurobiological processes. This improves mechanistic insight about both healthy white matter maturation and the developmental origins of white-matter pathologies.

With this study we explore the development of thalamocortical white matter by quantifying microstructure in the different layers of the fetal brain. Using diffusion metrics, we characterise the emergence of structural connectivity from the thalamus to spatially and functionally distinct cortical brain regions. We observe correlations between the transitioning tissue components and key neurobiological processes in white matter development. By providing a detailed normative reference of MR signal change during the second to third trimester, this will help future studies to identify if the tissue properties of specific compartments are affected by preterm birth or other perinatal injury. To this effect, all fetal MRI data is made available to the research community.

Materials and Methods

Sample

The study was approved by the UK Health Research Authority (Research Ethics Committee reference number: 14/LO/1169) and written parental consent was obtained in every case for imaging and open data release of the anonymized data.

Acquisition, pre-processing, and quality control

GA was determined by sonography at 12 post-ovulatory weeks as part of routine clinical care. 300 fetal MRI datasets were acquired with a Philips Achieva 3T system, with a 32-channel cardiac coil in maternal supine position. dMRI data was collected with a combined spin echo and field echo (SAFE) sequence (Hutter, Slator, et al. 2018, Cordero-Grande et al., 2018) at 2 mm isotropic resolution, using a multi-shell diffusion encoding that consists of 15 volumes at b= 0 s/mm^2 , 46 volumes at b= 400 s/mm^2 , and 80 volumes at b= 1000 s/mm^2 lasting 14 minutes (Christiaens et al., 2019). The protocol also included the collection of structural T2w, T1w, and fMRI data, for a total imaging time of approximately 45 minutes (Price at al., 2019).

dMRI data were processed using a bespoke pipeline (Christiaens et al., 2019) that includes Generalized Singular Value Shrinkage (GSVS) image denoising and debiasing from complex data (Cordero-Grande et al., 2019), dynamic distortion correction of susceptibility-induced B0 field changes using the SAFE information (Ghiglia 1994, Cordero-Grande et al., 2018, Hutter, Slator, et al. 2018) and slice-to-volume motion correction based on a multi-shell spherical harmonics and radial decomposition (SHARD) representation (Christiaens et al., 2021). Quality control was implemented using summary metrics based on the gradient of the motion parameters over time and the percentage of slice dropouts in the data (Christiaens et al., 2021). This was followed up with expert visual assessment, which considered any residual or uncorrected artefacts. Based on the above criteria, 140 of the 300 subjects that were pre-processed were classified as high-quality reconstructions for both DWI and T2 modalities. Both DWI and T2 for each fetus were required to facilitate co-registration to template space via a structural intermediate.

Diffusion modelling and template generation

All diffusion processing and tractography was done using MRtrix3 (Tournier 2019). To model the tissue and fluid components of the diffusion data, WM and CSF response functions were estimated for each

subject using T2-based tissue segmentations as inclusion areas. WM response functions were extracted from areas of relatively mature white matter (corticospinal tract and corpus callosum) using the "tournier" algorithm and CSF responses using the "dhollander" algorithm in MRtrix3 (Jeurissen et al. 2014; Tournier et al. 2019; Tournier, Calamante, and Connelly 2013, Dhollander 2019). The WM response functions of the oldest 20 subjects were averaged to obtain a group-average response function of relatively mature WM, whilst a group-average CSF response function was calculated from the whole cohort of subjects. dMRI signal of all subjects was subsequently deconvolved into tissue ODF and fluid components using MSMT-CSD and the group-average WM and CSF response functions (Jeurissen et al. 2014), and resulting components were intensity normalised for each subject (Raffelt et al. 2011). Subject ODFs warped into weekly templates through a series of coarse pose normalisation and nonlinear diffeomorphic image registration steps (Jenkinson 2002, Raffelt 2011, Pietsch 2019). These transformations were composed to obtain pairs of inverse consistent diffeomorphic subject-to-template and template-to subject warps.

Connectome generation & tractography

The ODF templates were co-registered to the Boston T2-fetal atlas (Gholipour et al. 2017) using non-linear registration (Avants, Tustison, and Johnson 2014). The tissue segmentations of the cortex, white matter and deep grey matter were used for anatomically constrained tractography to generate whole-brain structural connectomes of 100M streamlines in each gestational week (Smith et al. 2012; Tournier et al. 2019). The connectomes were filtered down to 10M streamlines using the SIFT algorithm (Smith et al. 2013; Tournier et al. 2019), so that the number of streamlines connecting the two regions are approximately proportional to the cross-sectional area of the fibres connecting them (Smith et al. 2013). In each weekly template, thalamocortical pathways of interest were defined in both hemispheres by filtering the connectome using seed regions derived from the Boston T2-fetal atlas (Gholipour et al. 2017), including the thalamus, primary motor cortex, primary sensory cortex, posterior parietal cortex, dorso-lateral prefrontal cortex, and primary visual cortex. We also used additional ROIs to exclude

449 spurious streamlines that were projecting away from the expected path of the tract (for example, to
450 exclude callosal fibres from the thalamic-motor tract).
451
452 **Tract-density parcellation of thalamus**
453
454 Tckmap was used to identify which voxels in the thalamus mask were traversed by the streamlines of
455 each tract (Calamante et al. 2010). The tract density maps were merged using FSL (Jenkinson et al.
456 2012) and a colour-coded parcellation volume was constructed reflecting the maximum density tract
457 for each voxel. For visualisation, the tract density maps for each tract were thresholded at 80%, only to
458 include voxels with the highest streamline connectivity.
459
460 **Extracting tissue and fluid fraction values**
461
462 To extract diffusion metrics for analysis, In parallel, tracts were transformed from the templates to
463 age-matched subject space to be overlaid onto the normalised fluid ODF, and the normalised tissue
464 ODF. The mean value within the segmented tracts was calculated to give the tissue and fluid
465 fractions.
466
467 **Microstructural profiling**
468
469 In each template, thalamocortical tracts were filtered so all the streamlines for each tract were the same
470 length, to ensure even sampling intervals along them. All template tracts were then registered into a
471 standard space and resampled to 100 points (Tournier et al. 2019), before being transformed to
472 individual subjects and overlaid on the normalised tissue and fluid fraction maps. The average value for
473 each sampling point was calculated to create a microstructural profile along the path between the
474 thalamus and the cortical plate. To provide a reference for microstructural differences between fetal
475 brain compartments, tracts were overlaid on the atlas-derived tissue parcellations. The value of the
476 tissue labels underlying the tract were used to establish which sampling points corresponded to each

fetal compartment. These boundaries between compartments were then used to label the plots in Figure 5.

Acknowledgements

We thank the patients who agreed to participate in this work and the staff of St. Thomas' Hospital London. This work was supported by the European Research Council under the European Union Seventh Framework Programme (FP/2007-2013)/ERC Grant Agreement No. 319456. We acknowledge infrastructure support from the National Institute for Health Research (NIHR) Mental Health Biomedical Research Centre (BRC) at South London and Maudsley NHS Foundation Trust, King's College London, and the NIHR-BRC at Guy's and St Thomas' NHS Foundation Trust. We also acknowledge grant support in part from the Wellcome Engineering and Physical Sciences Research Council (EPSRC) Centre for Medical Engineering at King's College London (WT 203148/Z/16/Z) and the Medical Research Council (UK) (MR/K006355/1 and MR/L011530/1). J.O. is supported by a Sir Henry Dale Fellowship jointly funded by the Wellcome Trust and the Royal Society (Grant 206675/Z/17/Z). J.O. and A.D.E. received support from the Medical Research Council Centre for Neurodevelopmental Disorders, King's College London (Grant MR/N026063/1). T.A. was supported by an MRC Clinician Scientist Fellowship (MR/P008712/1). Support for this work was also provided by the NIHR-BRC at Kings College London, Guy's and St Thomas' NHS Foundation Trust in partnership with King's College London, and King's College Hospital NHS Foundation Trust.

Competing interests

The authors declare no competing interests.

References

Anticevic, Alan et al. 2014. "Characterizing Thalamo-Cortical Disturbances in Schizophrenia and Bipolar Illness." *Cerebral Cortex* 24(12): 3116–30. https://academic.oup.com/cercor/article/24/12/3116/272693.

505 Avants, Brian B, Nick Tustison, and Hans Johnson. 2014. *Advanced Normalization Tools (ANTS)*
506 *Release 2.X*. https://brianavants.wordpress.com/2012/04/13/updated-ants-compile-instructions-
507 april-12-2012/ (June 23, 2021).
508 Back, Stephen A. et al. 2002. "Arrested Oligodendrocyte Lineage Progression during Human Cerebral
509 White Matter Development: Dissociation between the Timing of Progenitor Differentiation and
510 Myelinogenesis." *Journal of Neuropathology and Experimental Neurology* 61(2): 197–211.
511 https://pubmed.ncbi.nlm.nih.gov/11853021/ (January 25, 2021).
512 Back, Stephen A et al. 2001. "Late Oligodendrocyte Progenitors Coincide with the Developmental
513 Window of Vulnerability for Human Perinatal White Matter Injury." *Journal of Neuroscience*
514 21(4): 1302–12.
515 Ball, Gareth et al. 2013. "The Influence of Preterm Birth on the Developing Thalamocortical
516 Connectome." *Cortex* 49(6): 1711–21.
517 ———. 2015. "Thalamocortical Connectivity Predicts Cognition in Children Born Preterm."
518 *Cerebral Cortex* 25(11): 4310–18. https://pubmed.ncbi.nlm.nih.gov/25596587/ (August 16,
519 2022).
520 Brody, Betty Ann, Hannah C. Kinney, Alexander S. Kloman, and Floyd H. Gilles. 1987. "Sequence
521 of Central Nervous System Myelination in Human Infancy. I. An Autopsy Study of
522 Myelination." *Journal of Neuropathology and Experimental Neurology* 46(3): 283–301.
523 https://academic.oup.com/jnen/article-lookup/doi/10.1097/00005072-198705000-00005 (June
524 24, 2020).
525 Bui, Tony et al. 2006. "Microstructural Development of Human Brain Assessed in Utero by Diffusion
526 Tensor Imaging." *Pediatric Radiology* 36(11): 1133–40.
527 Calamante, Fernando, Jacques Donald Tournier, Graeme D. Jackson, and Alan Connelly. 2010.
528 "Track-Density Imaging (TDI): Super-Resolution White Matter Imaging Using Whole-Brain
529 Track-Density Mapping." *NeuroImage* 53(4): 1233–43.
530 Christiaens, D., Cordero-Grande, L., Price, A.N., Hutter, J., Hughes, E., Counsell, S.J., Tournier, J-D.,
531 Hajnal, J.V. (2019). Fetal diffusion MRI acquisition and analysis in the developing Human
532 Connectome Project. vol. 27, (Abstract No. 629). Presented at the ISMRM Annual Meeting &

Exhibition, Montréal, QC, Canada, 11 May 2019-16 May 2019.

Christiaens, Daan et al. 2019. "In Utero Diffusion MRI: Challenges, Advances, and Applications." *Topics in Magnetic Resonance Imaging* 28(5): 255–64. https://doi.org/10.1097/RMR.0000000000000211 (February 3, 2021).

Clascá, Francisco, Pablo Rubio-Garrido, and Denis Jabaudon. 2012. "Unveiling the Diversity of Thalamocortical Neuron Subtypes." *European Journal of Neuroscience* 35(10): 1524–32. https://onlinelibrary.wiley.com/doi/full/10.1111/j.1460-9568.2012.08033.x (July 5, 2022).

Cordero-Grande, L., Price, A.N., Ferrazzi, G., Hutter, J., Christiaens, D., Hughes, E., Hajnal, J.V. (2018). Spin And Field Echo (SAFE) dynamic field correction in 3T fetal EPI. vol. 26, (Abstract No. 208). Presented at the Joint Annual Meeting ISMRM-ESMRMB, Paris, France, 16 Jun 2018-21 Jun 2018.

Cordero-Grande, L., Christiaens, D., Hutter, J., Price, A.N., Hajnal, J.V. (2019). Complex diffusion-weighted image estimation via matrix recovery under general noise models. NeuroImage, 200, 391-404. doi: 10.1016/j.neuroimage.2019.06.039

Drobyshevsky, Alexander et al. 2005. "Developmental Changes in Diffusion Anisotropy Coincide with Immature Oligodendrocyte Progression and Maturation of Compound Action Potential." *Journal of Neuroscience* 25(25): 5988–97.

Emos, Marc Christopher, and Sanjeev Agarwal. 2019. StatPearls *Neuroanatomy, Internal Capsule*. StatPearls Publishing. https://www.ncbi.nlm.nih.gov/books/NBK542181/ (July 29, 2022).

Gholipour, Ali et al. 2017. "A Normative Spatiotemporal MRI Atlas of the Fetal Brain for Automatic Segmentation and Analysis of Early Brain Growth." *Scientific Reports* 7(1). www.nature.com/scientificreports.

Ghosh, Anirvan, Antonella Antonini, Susan K. McConnell, and Carla J. Shatz. 1990. "Requirement for Subplate Neurons in the Formation of Thalamocortical Connections." *Nature* 347(6289): 179–81. https://www.nature.com/articles/347179a0 (August 2, 2022).

Haynes, Robin L. et al. 2005. "Axonal Development in the Cerebral White Matter of the Human Fetus and Infant." *Journal of Comparative Neurology* 484(2): 156–67. https://pubmed.ncbi.nlm.nih.gov/15736232/ (February 19, 2021).

561 Huttenlocher, Peter R., and Arun S. Dabholkar. 1997. "Regional Differences in Synaptogenesis in
562 Human Cerebral Cortex." *Journal of Comparative Neurology* 387(2): 167–78.
563 https://onlinelibrary.wiley.com/doi/epdf/10.1002/%28SICI%291096-
564 9861%2819971020%29387%3A2%3C167%3A%3AAID-CNE1%3E3.0.CO%3B2-Z (August 3,
565 2022).
566 Hutter, Jana, Paddy J. Slator, et al. 2018. "Integrated and Efficient Diffusion-Relaxometry Using
567 ZEBRA." *Scientific Reports 2018 8:1* 8(1): 1–13. https://www.nature.com/articles/s41598-018-
568 33463-2 (August 19, 2022).
569 Hutter, Jana, Daan J. Christiaens, et al. 2018. "Slice-Level Diffusion Encoding for Motion and
570 Distortion Correction." *Medical Image Analysis* 48: 214–29.
571 https://europepmc.org/articles/PMC6191883 (June 24, 2020).
572 Jaimes, Camilo et al. 2020. "In Vivo Characterization of Emerging White Matter Microstructure in
573 the Fetal Brain in the Third Trimester." *Human Brain Mapping* 41(12): 3177–85.
574 https://onlinelibrary.wiley.com/doi/abs/10.1002/hbm.25006 (June 24, 2020).
575 Jakab, András et al. 2015. "Fetal Cerebral Magnetic Resonance Imaging Beyond Morphology."
576 *Seminars in Ultrasound, CT and MRI* 36(6): 465–75.
577 Jenkinson, Mark et al. 2012. "Review FSL." *NeuroImage* 62(2): 782–90.
578 https://research.utwente.nl/en/publications/fsl (June 23, 2020).
579 Jeurissen, Ben et al. 2014. "Multi-Tissue Constrained Spherical Deconvolution for Improved Analysis
580 of Multi-Shell Diffusion MRI Data." *NeuroImage* 103: 411–26.
581 Jones, Edward G. 2007. *The Thalamus*.
582 Keunen, Kristin et al. 2018. "Early Human Brain Development: Insights into Macroscale Connectome
583 Wiring." *Pediatric Research* 84(6): 829–36.
584 Khan, Shadab et al. 2019. "Fetal Brain Growth Portrayed by a Spatiotemporal Diffusion Tensor MRI
585 Atlas Computed from in Utero Images." *NeuroImage* 185(August 2018): 593–608.
586 Kinney, Hannah C. et al. 1994. "Myelination in the Developing Human Brain: Biochemical
587 Correlates." *Neurochemical Research* 19(8): 983–96.
588 https://link.springer.com/article/10.1007/BF00968708 (January 25, 2021).

589 Kinney, Hannah C., Betty Ann brody, Alexander S. Kloman, and Floyd H. Gilles. 1988. "Sequence of
590 Central Nervous System Myelination in Human Infancy. II. Patterns of Myelination in
591 Autopsied Infants." *Journal of Neuropathology and Experimental Neurology* 47(3): 217–34.
592 https://academic.oup.com/jnen/article-lookup/doi/10.1097/00005072-198805000-00003
593 (January 25, 2021).
594 Klingner, Carsten M et al. 2014. "Thalamocortical Connectivity during Resting State in
595 Schizophrenia." *European Archives of Psychiatry and Clinical Neuroscience* 264(2): 111–19.
596 http://www.fil.ion.
597 Kostović, I., and M. Judaš. 2015. "Embryonic and Fetal Development of the Human Cerebral
598 Cortex." *Brain Mapping: An Encyclopedic Reference* 2: 167–75.
599 Kostovic, I., and P. Rakic. 1984. "Development of Prestriate Visual Projections in the Monkey and
600 Human Fetal Cerebrum Revealed by Transient Cholinesterase Staining." *Journal of*
601 *Neuroscience* 4(1): 25–42. https://pubmed.ncbi.nlm.nih.gov/6693940/ (July 27, 2022).
602 Kostovic, Ivica, and Patricia S. Goldman-Rakic. 1983. "Transient Cholinesterase Staining in the
603 Mediodorsal Nucleus of the Thalamus and Its Connections in the Developing Human and
604 Monkey Brain." *Journal of Comparative Neurology* 219(4): 431–47.
605 https://onlinelibrary.wiley.com/doi/full/10.1002/cne.902190405 (July 27, 2022).
606 Kostović, Ivica, and Nataša Jovanov-Milošević. 2006. "The Development of Cerebral Connections
607 during the First 20-45 Weeks' Gestation." *Seminars in Fetal and Neonatal Medicine* 11(6): 415–
608 22. https://pubmed.ncbi.nlm.nih.gov/16962836/ (June 24, 2020).
609 Kostović, Ivica, and Miloš Judaš. 2006. "Prolonged Coexistence of Transient and Permanent Circuitry
610 Elements in the Developing Cerebral Cortex of Fetuses and Preterm Infants." *Developmental*
611 *Medicine and Child Neurology* 48(5): 388–93. http://www.ncbi.nlm.nih.gov/pubmed/16608549
612 (June 24, 2020).
613 ———. 2010. "The Development of the Subplate and Thalamocortical Connections in the Human
614 Foetal Brain." *Acta Paediatrica, International Journal of Paediatrics* 99(8): 1119–27.
615 Kostovic, Ivica, and Pasko Rakic. 1990a. "Developmental History of the Transient Subplate Zone in
616 the Visual and Somatosensory Cortex of the Macaque Monkey and Human Brain." *Journal of*

Comparative Neurology 297(3): 441–70.
https://onlinelibrary.wiley.com/doi/full/10.1002/cne.902970309 (July 27, 2022).

———. 1990b. "Developmental History of the Transient Subplate Zone in the Visual and Somatosensory Cortex of the Macaque Monkey and Human Brain." *The Journal of Comparative Neurology* 297(3): 441–70. http://doi.wiley.com/10.1002/cne.902970309 (December 24, 2019).

Krsnik, Željka et al. 2017. "Growth of Thalamocortical Fibers to the Somatosensory Cortex in the Human Fetal Brain." *Frontiers in Neuroscience* 11(APR): 233. www.frontiersin.org.

Lockwood Estrin, Georgia et al. 2019. "White and Grey Matter Development in Utero Assessed Using Motion-Corrected Diffusion Tensor Imaging and Its Comparison to Ex Utero Measures." *Magnetic Resonance Materials in Physics, Biology and Medicine* 32(4): 473–85.

Machado-Rivas, Fedel et al. 2021. "Spatiotemporal Changes in Diffusivity and Anisotropy in Fetal Brain Tractography." *Human Brain Mapping* 42(17): 5771–84.
https://onlinelibrary.wiley.com/doi/full/10.1002/hbm.25653 (August 3, 2022).

Marenco, Stefano et al. 2012. "Investigation of Anatomical Thalamo-Cortical Connectivity and FMRI Activation in Schizophrenia." *Neuropsychopharmacology* 37(2): 499.
/pmc/articles/PMC3242311/ (August 2, 2022).

Miyazaki, Yuta, Jae W. Song, and Emi Takahashi. 2016. "Asymmetry of Radial and Symmetry of Tangential Neuronal Migration Pathways in Developing Human Fetal Brains." *Frontiers in Neuroanatomy* 10(JAN).

Molliver, Mark E., Ivica Kostović, and Hendrik Van Der Loos. 1973. "The Development of Synapses in Cerebral Cortex of the Human Fetus." *Brain Research* 50(2): 403–7.

Molnár, Zoltán, and Colin Blakemore. 1995. "How Do Thalamic Axons Find Their Way to the Cortex?" *Trends in Neurosciences* 18(9): 389–97. https://pubmed.ncbi.nlm.nih.gov/7482804/ (August 2, 2022).

Morel, Anne, Michel Magnin, and Daniel Jeanmonod. 1997. "Multiarchitectonic and Stereotactic Atlas f the Human Thalamus." *Journal of Comparative Neurology* 387(4).

Nair, Aarti et al. 2013. "Impaired Thalamocortical Connectivity in Autism Spectrum Disorder: A Study of Functional and Anatomical Connectivity." *Brain* 136(6): 1942–55.

https://academic.oup.com/brain/article/136/6/1942/619231.

Najdenovska, Elena et al. 2018. "In-Vivo Probabilistic Atlas of Human Thalamic Nuclei Based on Diffusion-Weighted Magnetic Resonance Imaging." *Scientific Data* 5(1): 1–11. https://www.nature.com/articles/sdata2018270 (August 16, 2022).

Nakagawa, Yasushi. 2019. "Development of the Thalamus: From Early Patterning to Regulation of Cortical Functions." *Wiley Interdisciplinary Reviews: Developmental Biology* 8(5): e345. https://onlinelibrary.wiley.com/doi/full/10.1002/wdev.345 (July 5, 2022).

Niemann, K., V. R. Mennicken, D. Jeanmonod, and A. Morel. 2000. "The Morel Stereotactic Atlas of the Human Thalamus: Atlas-to-MR Registration of Internally Consistent Canonical Model." *NeuroImage* 12(6): 601–16.

Peter R., Huttenlocher. 1979. "Synaptic Density in Human Frontal Cortex - Developmental Changes and Effects of Aging." *Brain Research* 163(2): 195–205.

Pietsch, Maximilian et al. 2019. "A Framework for Multi-Component Analysis of Diffusion MRI Data over the Neonatal Period." *NeuroImage* 186: 321–37.

Price, David J. et al. 2006. "The Development of Cortical Connections." *European Journal of Neuroscience* 23(4): 910–20. https://onlinelibrary.wiley.com/doi/full/10.1111/j.1460-9568.2006.04620.x (August 2, 2022).

Price, A.N., Cordero-Grande, L., Hughes, E., Hiscocks, S., Green, E., McCabe, L., Hutter, J., Ferrazzi, G., Deprez, M., Roberts, T., Christiaens, D., Duff, E., Karolis, V., Malik, S., Rutherford, M., Edwards, A.D., Hajnal, J.V. (2019). The developing Human Connectome Project (dHCP): fetal acquisition protocol. vol. 27, (Abstract No. 244). Presented at the ISMRM Annual Meeting & Exhibition, Montréal, QC, Canada, 11 May 2019-16 May 2019.

Raffelt, David et al. 2011. "Symmetric Diffeomorphic Registration of Fibre Orientation Distributions." *NeuroImage* 56(3): 1171–80. https://pubmed.ncbi.nlm.nih.gov/21316463/ (June 25, 2020).

Schummers, James, Jitendra Sharma, and Mriganka Sur. 2005. "Bottom-up and Top-down Dynamics in Visual Cortex." In *Progress in Brain Research*, Elsevier, 65–81.

Sharma, Jitendra, Alessandra Angelucci, and Mriganka Sur. 2000. "Induction of Visual Orientation

673 Modules in Auditory Cortex." *Nature* 404(6780): 841–47.
674 https://www.nature.com/articles/35009043 (August 2, 2022).
675 Smith, Robert E., Jacques Donald Tournier, Fernando Calamante, and Alan Connelly. 2012.
676 "Anatomically-Constrained Tractography: Improved Diffusion MRI Streamlines Tractography
677 through Effective Use of Anatomical Information." *NeuroImage* 62(3): 1924–38.
678 ———. 2013. "SIFT: Spherical-Deconvolution Informed Filtering of Tractograms." *NeuroImage* 67:
679 298–312.
680 Sur, Mriganka, and John L.R. Rubenstein. 2005. "Patterning and Plasticity of the Cerebral Cortex."
681 *Science (New York, N.Y.)* 310(5749): 805–10. https://pubmed.ncbi.nlm.nih.gov/16272112/ (July
682 5, 2022).
683 Takahashi, Emi, Rebecca D Folkerth, Albert M Galaburda, and Patricia E Grant. 2012. "Emerging
684 Cerebral Connectivity in the Human Fetal Brain: An MR Tractography Study." *Cerebral Cortex*
685 22(2): 455–64. https://academic.oup.com/cercor/article-abstract/22/2/455/340633 (June 24,
686 2020).
687 Toulmin, Hilary et al. 2021. "Functional Thalamocortical Connectivity at Term Equivalent Age and
688 Outcome at 2 Years in Infants Born Preterm." *Cortex* 135: 17–29.
689 Tournier, J. Donald et al. 2019. "MRtrix3: A Fast, Flexible and Open Software Framework for
690 Medical Image Processing and Visualisation." *NeuroImage* 202.
691 Wilkinson, Molly, Tara Kane, Rongpin Wang, and Emi Takahashi. 2017. "Migration Pathways of
692 Thalamic Neurons and Development of Thalamocortical Connections in Humans Revealed by
693 Diffusion MR Tractography." *Cerebral Cortex* 27(12): 5683–95.
694 https://academic.oup.com/cercor/article/27/12/5683/2629223.
695 Wilson, Siân et al. 2021. "Development of Human White Matter Pathways in Utero over the Second
696 and Third Trimester." *Proceedings of the National Academy of Sciences of the United States of*
697 *America* 118(20): 2023598118. https://www.pnas.org/content/118/20/e2023598118 (June 21,
698 2021).
699 Xu, Gang et al. 2014. "Radial Coherence of Diffusion Tractography in the Cerebral White Matter of
700 the Human Fetus: Neuroanatomic Insights." *Cerebral Cortex* 24(3): 579–92.

https://pubmed.ncbi.nlm.nih.gov/23131806/ (February 19, 2021).

Yakovlev, P. I., S. Locke, D. Y. Koskoff, and R. A. Patton. 1960. "Limbic Nuclei of Thalamus and Connections of Limbic Cortex." *Archives of Neurology* 3(6): 620–41. https://jamanetwork.com/journals/jamaneurology/fullarticle/562977 (August 2, 2022).

Zanin, Emilie et al. 2011. "White Matter Maturation of Normal Human Fetal Brain. An in Vivo Diffusion Tensor Tractography Study." *Brain and Behavior* 1(2): 95–108. http://doi.wiley.com/10.1002/brb3.17 (May 4, 2020).

zljak, Ladislav, Harry B.M. Uylings, Ivica Kostovic, and Corbert G. van Eden. 1992. "Prenatal Development of Neurons in the Human Prefrontal Cortex. II. A Quantitative Golgi Study." *Journal of Comparative Neurology* 316(4): 485–96. https://onlinelibrary.wiley.com/doi/full/10.1002/cne.903160408 (August 3, 2022).

Supplementary Information

Supplementary Figure 1.

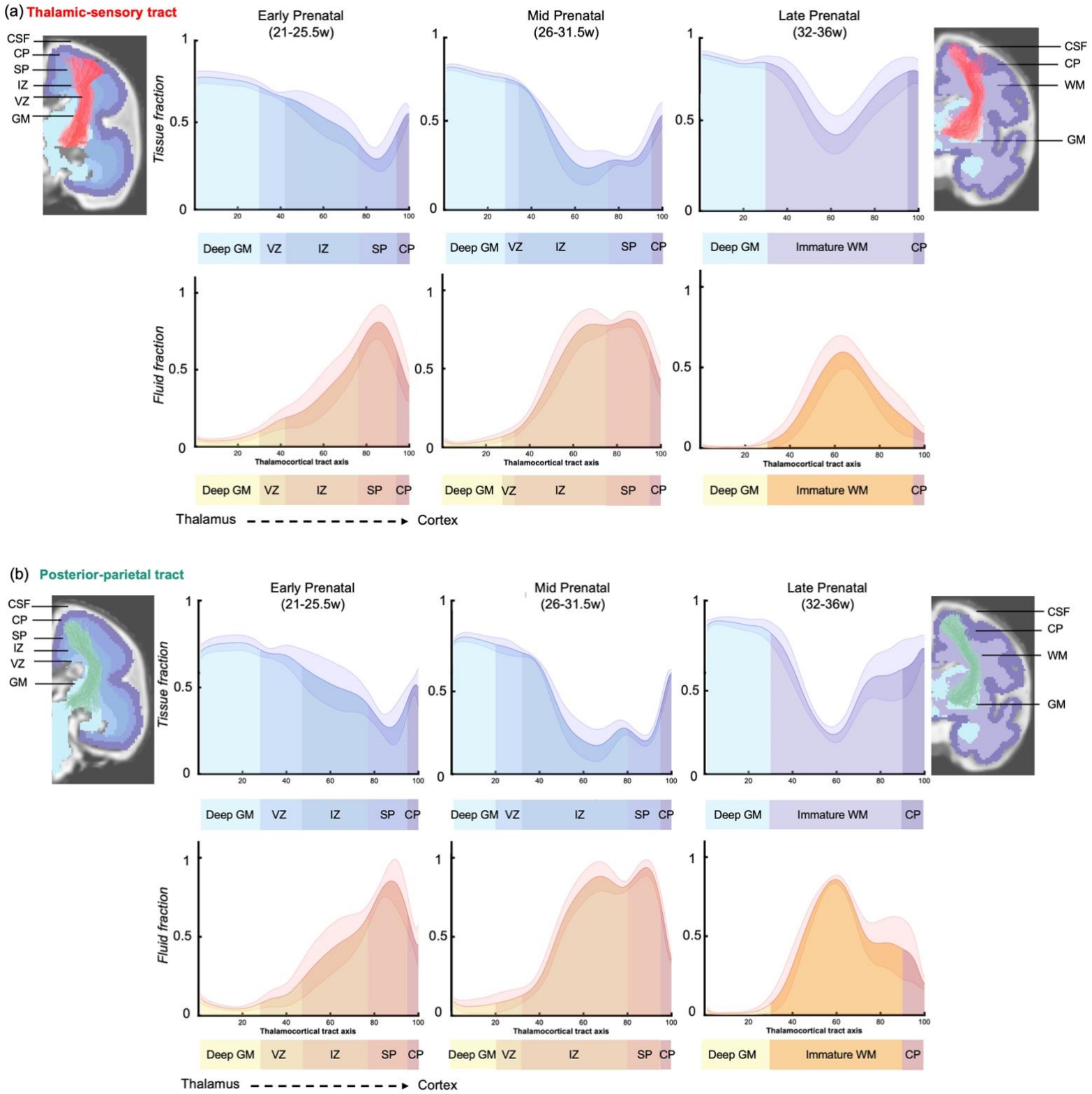

Supplementary Figure 1. Microstructural composition of fetal compartments traversed by developing thalamic white matter. *(a) Thalamic-sensory tract & (b) Posterior- parietal tract. Tracts were overlayed on the atlas of fetal compartments (examples highlight the difference between fetal brain structure in early prenatal (25w) on far left, and late prenatal (35w) on far right). Tissue fraction trends (top row) and fluid fraction trends (bottom row), normalised to 1, between the thalamus and cortex (thalamocortical tract axis). Subjects were grouped by age, and average trajectories plotted for early prenatal (22-25.5w), mid prenatal (26-31.5w), late prenatal (32-36w). Error bars represent the standard deviation among all subjects in each group. Atlas-derived tissue boundaries are marked on the trajectories to reveal the changing tissue properties of each layer between early, mid and late prenatal development. (Cortical spinal fluid = CSF, Cortical plate = CP, Subplate = SP, Intermediate zone = IZ, Ventricular zone = VZ, Deep grey matter = GM, Immature white matter = WM).*

Supplementary Figure 2 (a)

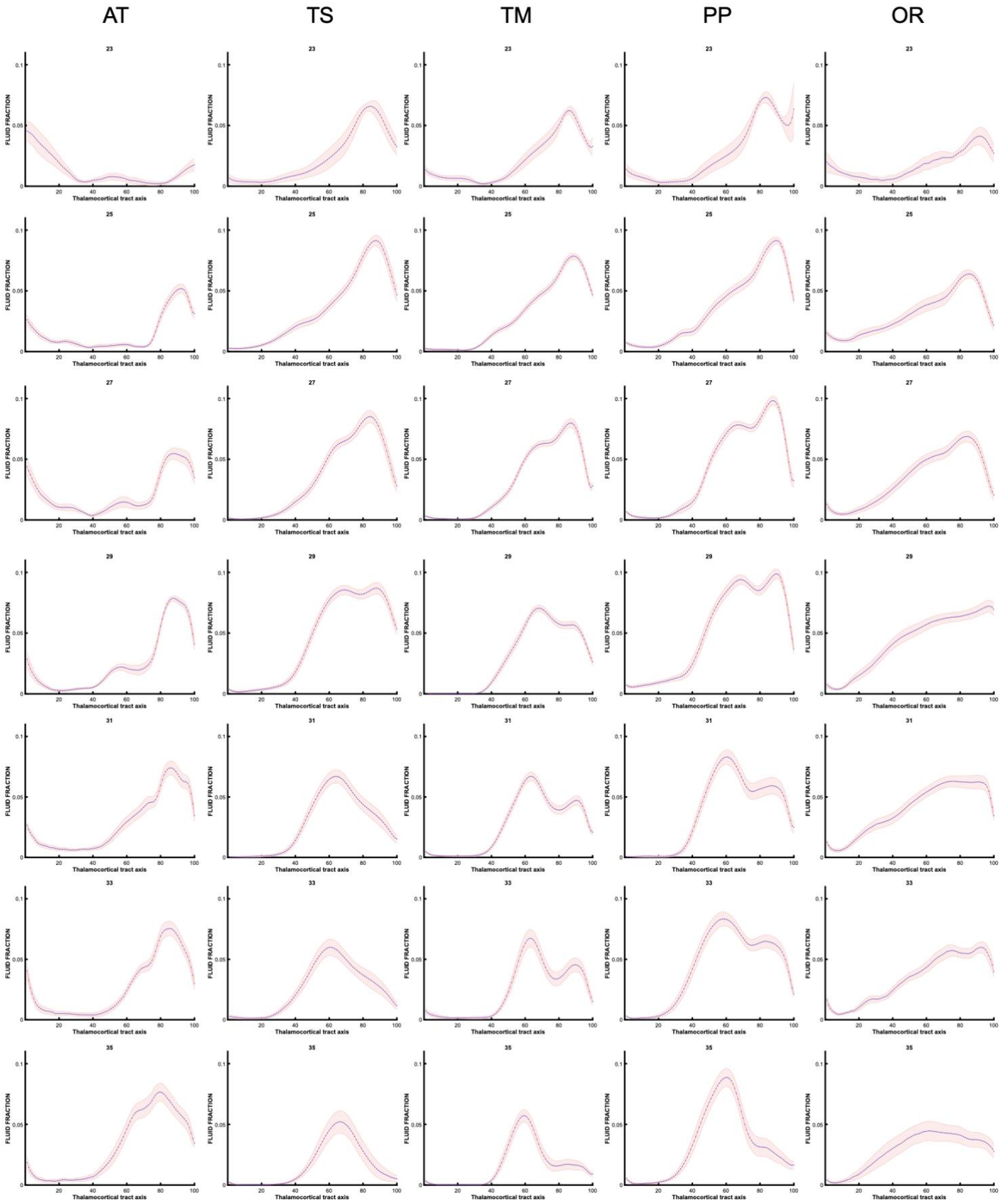

(b)

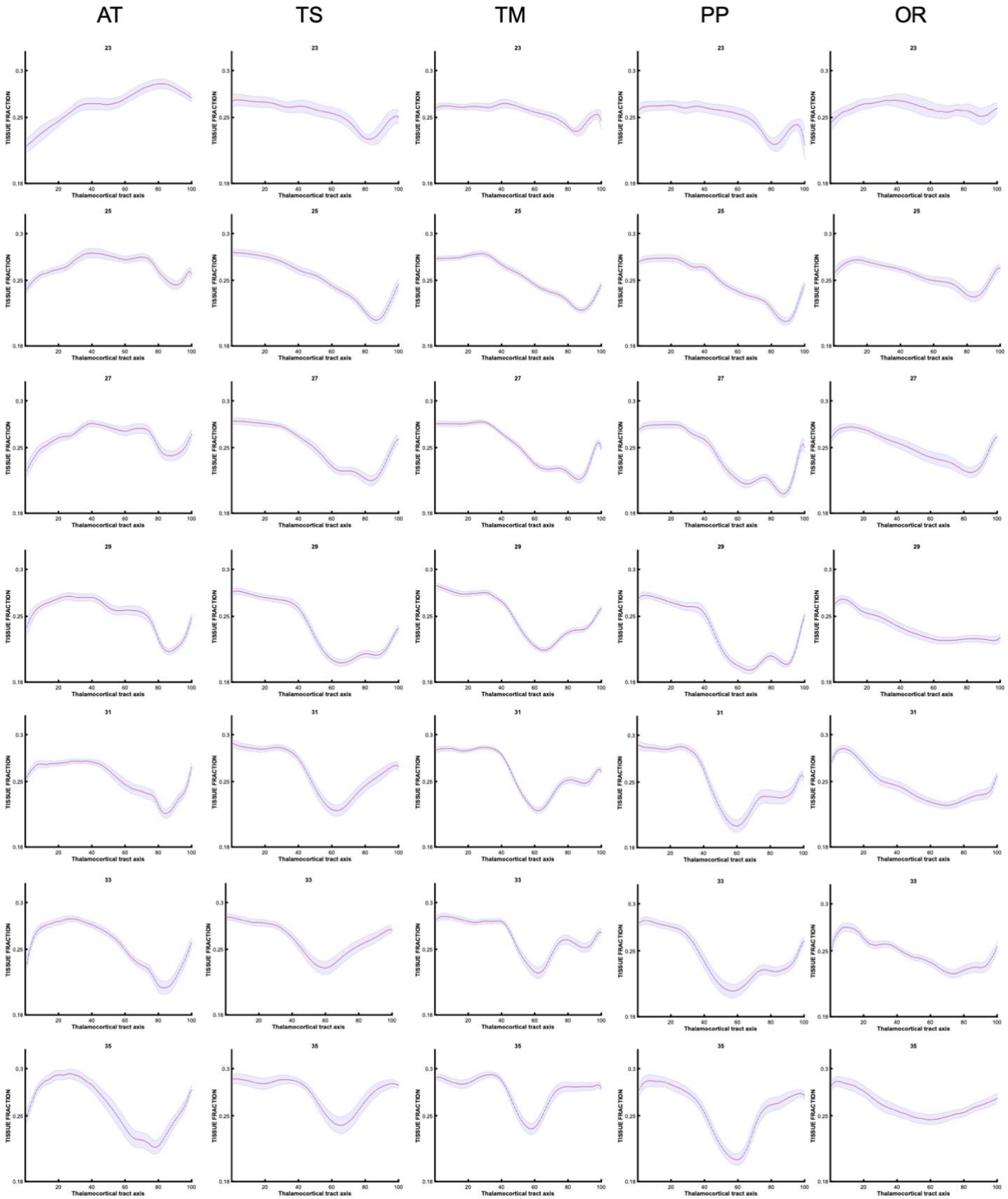

Supplementary Figure 2. Trajectories of fluid (a) and tissue (b) fraction along the thalamocortical axis for subjects in each gestational week (every other week shown)

Supplementary Figure 3.

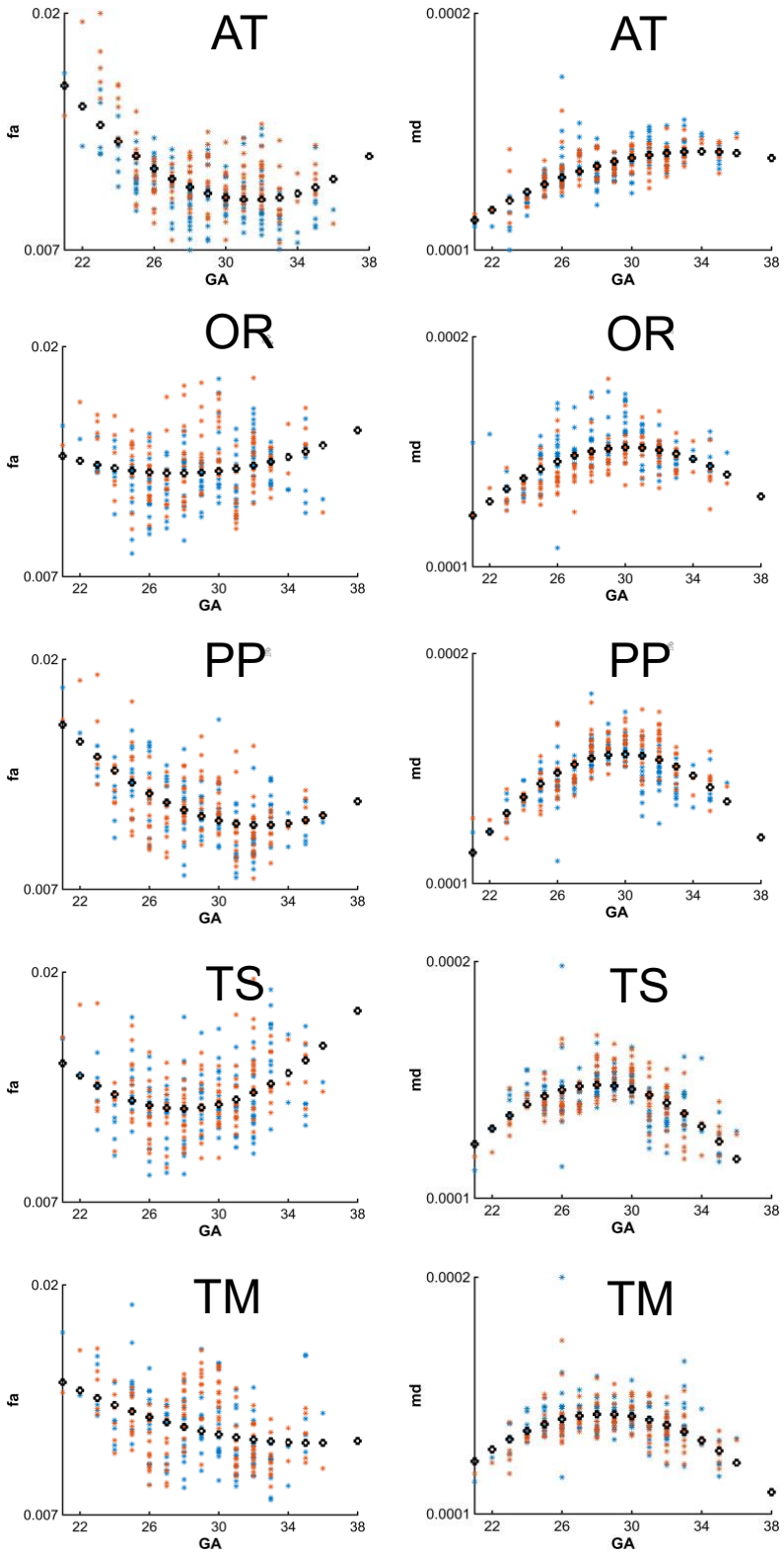

Supplementary Figure 3.

Diffusion tensor metric age-trajectories for each tract *(a) Whole-tract average fractional anisotryop (FA) and mean diffusivity (MD) for each subject in the left (orange) and right (blue) hemisphere, plotted against gestational age (GA) of the subject, best fit by 2nd order polynomials (AT = anterior thalamic radiation, OR = optic radiation, PP = posterior parietal tract, TS = thalamic-sensory tract, TM = thalamic-motor tract).*